

See discussions, stats, and author profiles for this publication at: <https://www.researchgate.net/publication/50418541>

# Distinct Binding Properties Distinguish LQ-Type Calmodulin-Binding Domains in Cyclic Nucleotide-Gated Channels

ARTICLE *in* BIOCHEMISTRY · MARCH 2011

Impact Factor: 3.02 · DOI: 10.1021/bi200115m · Source: PubMed

---

CITATIONS

10

---

READS

30

6 AUTHORS, INCLUDING:



**Jana Broecker**

University of Toronto

17 PUBLICATIONS 196 CITATIONS

SEE PROFILE



**Sandro Keller**

Technische Universität Kaiserslautern

90 PUBLICATIONS 1,302 CITATIONS

SEE PROFILE



**Frank Möhrle**

Universität Heidelberg

28 PUBLICATIONS 869 CITATIONS

SEE PROFILE

# Distinct Binding Properties Distinguish LQ-Type Calmodulin-Binding Domains in Cyclic Nucleotide-Gated Channels

Nicole Ungerer,<sup>†</sup> Norbert Mücke,<sup>‡</sup> Jana Broecker,<sup>§,⊥</sup> Sandro Keller,<sup>§,⊥</sup> Stephan Frings,<sup>†</sup> and Frank Möhrle<sup>\*,†</sup>

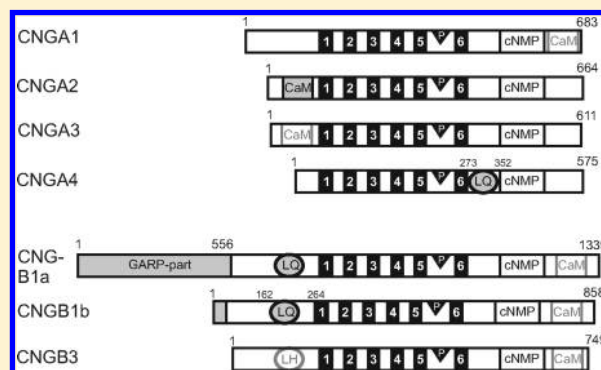
<sup>†</sup>Department of Molecular Physiology, University of Heidelberg, 69120 Heidelberg, Germany

<sup>‡</sup>Division of Biophysics of Macromolecules, German Cancer Research Center, 69120 Heidelberg, Germany

<sup>§</sup>Molecular Biophysics, University of Kaiserslautern, 67663 Kaiserslautern, Germany

<sup>⊥</sup>Biophysics of Membrane Proteins, Leibniz Institute of Molecular Pharmacology (FMP), 13125 Berlin, Germany

**ABSTRACT:** Cyclic nucleotide-gated (CNG) channels operate as transduction channels in photoreceptors and olfactory receptor neurons. Direct binding of cGMP or cAMP opens these channels which conduct a mixture of monovalent cations and  $\text{Ca}^{2+}$ . Upon activation, CNG channels generate intracellular  $\text{Ca}^{2+}$  signals that play pivotal roles in the transduction cascades of the visual and olfactory systems. Channel activity is controlled by negative feedback mechanisms that involve  $\text{Ca}^{2+}$ -calmodulin, for which all CNG channels possess binding sites. Here we compare the binding properties of the two LQ-type calmodulin binding sites, both of which are thought to be involved in channel regulation. They reside on the isoforms CNGB1 and CNGB3. The CNGB1 subunit is present in rod photoreceptors and olfactory receptor neurons. The CNGB3 subunit is only expressed in olfactory receptor neurons, and there are conflicting results as to its role in calmodulin-mediated feedback inhibition. We examined the interaction of  $\text{Ca}^{2+}$ -calmodulin with two recombinant proteins that encompass either of the two LQ sites. Comparing binding properties, we found that the LQ site of CNGB1 binds  $\text{Ca}^{2+}$ -calmodulin at 10-fold lower  $\text{Ca}^{2+}$  levels than the LQ site of CNGB3. Our data provide biochemical evidence against a contribution of CNGB3 to feedback inhibition. In accordance with previous work on photoreceptor CNG channels, our results indicate that feedback control is the exclusive role of the B-subunits in photoreceptors and olfactory receptor neurons.



In mammals, cyclic nucleotide-gated channels are encoded by six genes *cnga1*, *cnga2*, *cnga3*, *cnga4*, *cnbg1*, and *cnbg3* which are mainly expressed in neurons.<sup>1–5</sup> The resulting proteins coassemble as tetramers with cell-specific stoichiometry which is best established for the transduction channels of rod photoreceptors (3 CNGB1 + 1 CNGB1a),<sup>6,7</sup> cone photoreceptors (2 CNGB3 + 2 CNGB3),<sup>8</sup> and olfactory receptor neurons (2 CNGB2 + 1 CNGB4 + 1 CNGB1b).<sup>9</sup> Besides the polarized expression of CNG channels in the sensory organelles (photoreceptor outer segment, olfactory sensory cilia) and their opening by the second messengers of vision (cGMP) and olfaction (cAMP), their ability to conduct  $\text{Ca}^{2+}$  into the cells is a particular focus of research. Various  $\text{Ca}^{2+}$ -induced processes are central components of the respective transduction pathways and have been studied in detail.<sup>10–12</sup> All CNG channels conduct  $\text{Ca}^{2+}$ , but the extent of their  $\text{Ca}^{2+}$  permeability critically depends on their subunit composition.<sup>13,14</sup> One modulatory mechanism common to all of them is the feedback inhibition mediated by calmodulin (CaM). Inflowing  $\text{Ca}^{2+}$  binds to calmodulin which then desensitizes the CNG channel to its ligand.<sup>15–19</sup> This process was first discovered in olfactory channels which show the most

pronounced desensitization response to calmodulin.<sup>20</sup> Homomeric CNGB2 channels bind calmodulin in a strictly  $\text{Ca}^{2+}$ -dependent way at an N-terminal binding site. This site is a classical amphipathic  $\alpha$ -helix with a 1–5–8–14 pattern of nonpolar residues interspaced with charged amino acids.<sup>19</sup> Binding of  $\text{Ca}^{2+}$ -calmodulin to CNGB2 depends on the closed state of the channel and causes desensitization by neutralizing an autoexcitatory domain.<sup>15</sup> In contrast, in olfactory channels that contain CNGB2 and the modulatory subunits CNGB4 and CNGB1b (the olfactory splice variant of CNGB1), feedback inhibition is neither state-dependent nor mediated by the CNGB2 site. Instead, an N-terminal LQ site of CNGB1b is necessary for desensitization.<sup>21–23</sup> LQ sites, like “IQ-type” calmodulin recognition motifs, bind calmodulin at very low  $\text{Ca}^{2+}$  concentrations.<sup>24</sup> Moreover, patch-clamp studies revealed that a second LQ site, which resides on the CNGB4 subunit, was needed for feedback inhibition in channels excised from cells and

**Received:** January 24, 2011

**Revised:** March 16, 2011

**Published:** March 17, 2011

washed with  $\text{Ca}^{2+}$ -free solution<sup>21</sup> but is not needed when cytosolic constituents are left on the channels.<sup>25</sup> Finally, calmodulin is permanently tethered to the channel at  $\text{Ca}^{2+}$  concentrations  $\geq 0.1 \mu\text{M}$ , showing a much stronger association with the heteromeric channel at low  $\text{Ca}^{2+}$  levels than with homomeric CNGA2 channels. Taken together, these various aspects of channel function suggest that several modes of calmodulin-mediated activity regulation can operate in CNG channels, depending on subunit composition and experimental conditions.

To approach a mechanistic concept for the roles of the modulatory subunits in feedback control, we addressed the controversial topic of CaM regulation in olfactory CNG channels. We examine the question whether the two LQ-type sites in CNGA4 and CNGB1b have similar or different calmodulin-binding properties. We generated recombinant proteins that contained the binding sites and studied their association with calmodulin, its  $\text{Ca}^{2+}$  dependence, and the complex formation of each protein with calmodulin.

## EXPERIMENTAL PROCEDURES

**Cloning of CNG Channel CaM Binding Proteins, OMP Control Protein, CaM<sup>12</sup>, CaM<sup>34</sup>, CaM<sup>1234</sup>, and CaM<sup>T35C</sup> in pET28a(+).** DNA was amplified by the Phusion High-Fidelity Taq-Polymerase (Finnzymes, Finland). Coding DNA of the CaM binding domains CNGA4<sup>N273-N351</sup> (A4) and CNGB1b<sup>A162-D264</sup> (B1b) was amplified from CNGA4 (GeneID: 85258; NM\_053496.2) and CNGB1b (GeneID: 83686, NM\_031809) in pcDNA3.1(+).<sup>25</sup> The primer pairs were for CaMA4<sup>N273-N351</sup> 5'-AAG CAT ATG AAC ACT GCA GAT GCG GCC TTC-3', and 5'-AAG GAT CCT CAA CAG TTC TGG AAG ATC TGT AC-3' and for CNGB1b<sup>A162-D264</sup> 5'-AAG CAT ATG GCT GAT GGC GAG GAC CGT GC-3' and 5'-AAG GAT CCT TAG TCG ATG CTC TGG GGG AAC T-3'. Wild-type CaM and the CaM mutants CaM<sup>12</sup>, CaM<sup>34</sup>, and CaM<sup>1234</sup> in pcDNA3<sup>26</sup> were provided by D.T. Yue (Johns Hopkins University School of Medicine, Baltimore, MA). EF-hand  $\text{Ca}^{2+}$  binding sites of CaM were disabled by D → A exchanges: EF-hand 1: D20A; EF-hand 2: D56A; EF-hand 3: D93A; EF-hand 4: D129A.<sup>27</sup> Primer pairs for PCR amplification were 5'-AAC TTAAGCATA TGA TGG CTG ACC AAC TGA CTG AAG-3' and 5'-AGG ATC CTC ACT TCG CTG TCA TCA TTT GTA C-3'. After PCR amplification and enzymatic digestion with *Bam*HI and *Nde*I, PCR products were directly subcloned in pET28a(+). For CaM<sup>T35C</sup> T → C exchange, site-directed mutagenesis was carried out using the Quick Change II XL Site-Directed Mutagenesis Kit (Stratagene, Netherlands) according to manufacturer's instructions. For cloning of the olfactory marker protein (OMP), total RNA from the olfactory epithelium (obtained from 3–6 month old Wistar rats, Charles River Laboratory, Germany) was amplified by RT-PCR and cloned in pET28a(+) with *Not*I and *Bam*HI using standard protocols. Primer pairs were 5'-AAG GAT CCA TGG CAG AGG ACG GGC CAC-3' and 5'-ATT GCG GCC GCT CAG AGC TGG TTA AAC ACC-3'. Correct plasmid identity was confirmed by sequencing.

**Expression and Purification of His<sub>6</sub>-Tagged Fusion Proteins.** Expression in pET28a(+) results in N-terminally His<sub>6</sub>-tagged fusion proteins. After expression in *E. coli* BL21 (DE3) pLys (Stratagene, Netherlands) proteins were purified on a His Trap FF column (GE Healthcare) according to Sambrook et al. (1989). Proteins were subjected to SDS-PAGE and standard

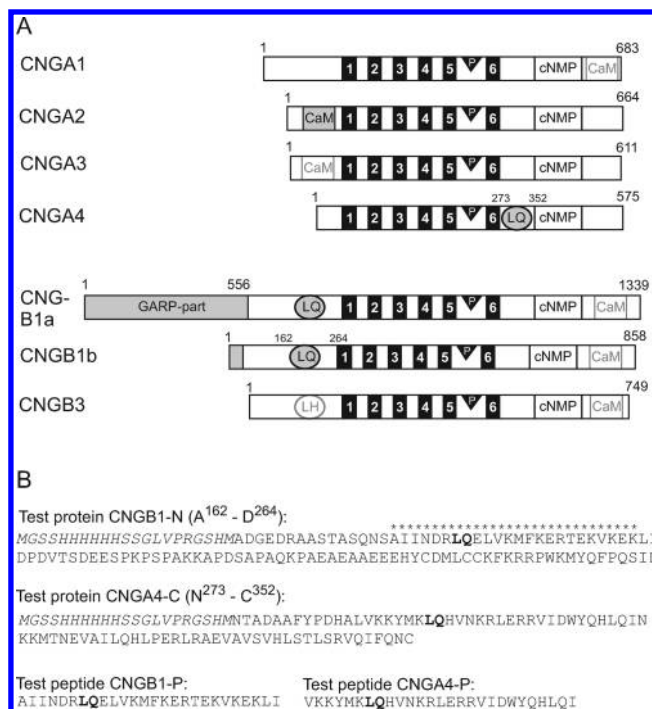


**Figure 1.** (A) Schematic representation of CNG channel subunits from rod photoreceptors (CNGA1, CNGB1a), cone photoreceptors (CNGA3, CNGB3), and olfactory receptor neurons (CNGA2, CNGA4, CNGB1b). The transmembrane domains are indicated by numbers. The pore loop (P) is located between transmembrane domains 5 and 6. Functional regions for channel regulation: the cyclic nucleotide binding sites (cNMP), the calmodulin-binding sites of the "IQ-type" motif class (LQ), and "Baa type" motifs (CaM). "Baa type" motifs that alone do not support physiological channel regulation (see text for details) and a site lacking critical signature residues of "IQ-type" sequences (LH in CNGB3) are depicted in gray. (B) Amino acid sequence of the test proteins CNGB1-N and CNGA4-C and of the test peptides CNGB1-P and CNGA4-P, respectively. For purification purposes the expressed proteins contained an N-terminal His<sub>6</sub>-tag (italic). Asterisks indicate predicted  $\alpha$ -helical regions identified by the Secondary Structure Prediction Server GOR IV (helix probability  $>0.750$ ).<sup>44</sup>

Coomassie stained. The identity of the fusion proteins was further confirmed by Western blotting on poly(vinylidene difluoride) membranes (Machery & Nagel, Germany) using mouse anti-His<sub>6</sub> as primary antibody (Qiagen, Germany) and the adequate horseradish peroxidase-conjugated secondary antibody (Sigma, Germany). The resulting chemiluminescence was detected with the ECL plus enhanced chemiluminescence system (GE Healthcare). Fusion proteins were dialyzed against distilled water and lyophilized.

**Peptides and Wild-Type Calmodulin.** Peptide synthesis was carried out at Peptide Specialty Laboratories, Heidelberg, Germany. The peptides represent the LQ-type calmodulin-binding site of the CNGB1 and CNGA4 subunit (Figure 1). Wild-type calmodulin was purchased from Merck (#208690, Merck, Germany).

**BADAN-Labeling of CaM<sup>T35C</sup>.** Reduction of cysteine prior to coupling was performed for 5 min in 0.5 mL of 20 mM Tris/HCl pH 7.4, 0.3 M KCl, 4 mM TCEP (tris(2-carboxyethyl)phosphine). For fluorescence labeling with BADAN (6-bromoacetyl-2-dimethylaminonaphthalene)<sup>28</sup> 0.5 mL of a 10-fold molar excess of label in *N,N*-dimethylformamide (DMF) was added dropwise. The

reaction was carried out for 4 h at room temperature in the dark, while shaking and stopped upon addition of  $\beta$ -mercaptoethanol to a final concentration of 30 mM. To avoid precipitation and dialysis tube damage, 9 mL of Tris pH 7.4 was added before dialysis against distilled water and lyophilization. The coupling efficiency was confirmed by standard Native PAGE (acrylamide concentration  $T = 15\%$ ,  $C = 3\%$ ) according to Lämmli (1979).

**Fluorescence Spectroscopy.** Steady-state fluorescence with  $\text{CaM}^{\text{BADAN}}$  was obtained on a Perkin-Elmer LS50 spectrofluorimeter in quartz cuvettes (Hellma, Germany) in a sample volume of 100  $\mu\text{L}$ . Fluorescence emission spectra were recorded between 400 and 600 nm after excitation at 387 nm (bandwidth 5–10 nm, scan speed 200 nm/min). Stock solutions of labeled proteins were made in buffer A (20 mM Tris, 100 mM NaCl, 10 mM EGTA, pH 7.2). Protein concentrations were determined spectrophotometrically with  $\epsilon_{386\text{ nm}}$  ( $\text{CaM}^{\text{BADAN}}$ ) = 20 100  $\text{M}^{-1}\text{ cm}^{-1}$  and  $\epsilon_{280\text{ nm}}$  (CNGA4<sup>N273-N351</sup>) = 10 030  $\text{M}^{-1}\text{ cm}^{-1}$  and  $\epsilon_{280\text{ nm}}$  (CNGB1b<sup>A162-D264</sup>) = 8670  $\text{M}^{-1}\text{ cm}^{-1}$  and additionally by Bradford assay. The final concentration was 1.5  $\mu\text{M}$  for  $\text{CaM}^{\text{BADAN}}$  and 3.0  $\mu\text{M}$  for unlabeled proteins.  $\text{CaM}^{\text{BADAN}}$  spectra were recorded in the presence or absence of protein at various  $\text{Ca}^{2+}$  concentrations, generated by different ratios of buffers A and B (buffer A supplemented with 10 mM  $\text{CaCl}_2$ ) according to ref 29. The free  $\text{Ca}^{2+}$  concentration was calculated using WINMAX v2.50. All experiments were done at room temperature.

**Circular Dichroism Spectroscopy.** Far-UV circular dichroism (CD) spectra from 190 to 260 nm were recorded with a Jasco (Gross-Umstadt, Germany) J-720 spectropolarimeter at 25 °C in quartz cuvettes (Hellma, Germany) in a sample volume of 200  $\mu\text{L}$ , averaging three scans with the buffer baseline subtracted (step size 0.1 nm, scan speed 100 nm/min). Stock solutions of proteins were made in buffer A, containing 30  $\mu\text{M}$   $\text{Ca}^{2+}$ . Protein concentrations were 20  $\mu\text{M}$  each. For spectra analysis the program CD Mix was used, kindly provided by S. Keller (FMP, Berlin, Germany). For curve fitting data points were converted from millidegrees (mdeg) to mean residue ellipticity (%mR). The secondary structure content of proteins were estimated by decomposing the CD curves into basic spectra representing  $\alpha$ -helices,  $\beta$ -sheets, turns, and random-coil conformations in proteins.<sup>30</sup> All experiments were done at room temperature.

**Analytical Ultracentrifugation.** Sedimentation velocity experiments were performed in a Beckman analytical ultracentrifuge (Optima XLA) in double sector charcoal Epon cells at 20 °C at 60 000 rpm. Absorbance versus radius data were recorded at 230 nm using a spacing of 0.1 cm with four averages in a continuous scan mode. Data were analyzed with DCDT+, v.2.2. Protein concentrations were 9  $\mu\text{M}$  calmodulin and 18  $\mu\text{M}$  CNGA4-C and CNGB1-N. Solutions of calmodulin, calmodulin + CNGB1-N, and calmodulin + CNGA4-C were made in buffer C (20 mM Tris, 100 mM NaCl, pH 7.2) containing 1 mM  $\text{CaCl}_2$ . Densities and viscosities of the buffer and molar extinction coefficients,  $\epsilon$ , of proteins were calculated using the program SEDNTERP v1.07. All experiments were done at room temperature.

## RESULTS

All CNG-channel subunits possess putative calmodulin-binding sites (Figure 1A), but not all of these sites have been shown to participate in channel regulation. In rod photoreceptor channels (3 CNGA1 + 1 CNGB1a), the  $\text{Ca}^{2+}$  sensitivity appears to be mediated exclusively by the N-terminal LQ-site in CNGB1a.<sup>16,17,31</sup> No information is available on any functional

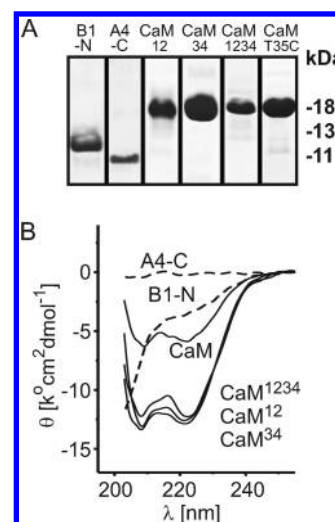


**Figure 2.** (A) Coomassie stained SDS-PAGE demonstrating the homogeneity of the purified proteins used in this study. The predicted molecular weights are  $\text{CaM}^{\text{T35C}}$ : 19.1 kDa;  $\text{CaM}^{12}$ ,  $\text{CaM}^{34}$ , and  $\text{CaM}^{1234}$ : 19.0 kDa; CNGB1-N: 13.9 kDa; CNGA4-C: 11.8 kDa. (B) Far-UV CD spectra of the purified proteins and wild-type calmodulin. Typical of extensive  $\alpha$ -helical structure are two minima at 208 and 222 nm, as apparent in the W-shaped curves of all calmodulins. The spectra of CNGB1-N (B1-N) indicate high random-coil content, characterized by a minimum around 200 nm, and low absolute intensity at 222 nm, with some residual  $\alpha$ -helical structure. The CD spectra of CNGA4-C (A4-C) display only little ellipticity, which is diagnostic of unordered regions.

significance of the two C-terminal binding sites in the A and B subunits. Similarly, in cone photoreceptor CNG channels (2 CNGA3 + 2 CNGB3),  $\text{Ca}^{2+}$  sensitivity is conferred by the B subunits. Both the N-terminal and C-terminal sites of CNGB3 are necessary to render the channel  $\text{Ca}^{2+}$ -sensitive.<sup>32</sup> The olfactory CNG channel (2 CNGA2 + 1 CNGA4 + 1 CNGB1b) appears to be an exception to the rule that only B-subunits mediate feedback inhibition in this channel family. While the N-terminal LQ site of CNGB1b certainly contributes to  $\text{Ca}^{2+}$ -dependent regulation,<sup>21,23</sup> the subunit CNGA4 was reported to be involved as well,<sup>21</sup> albeit only after the channels were extensively washed in  $\text{Ca}^{2+}$ -free solution.<sup>25</sup> This puzzling observation raises the question whether the LQ sites of CNGB1b and CNGA4 represent equivalent calmodulin-binding domains. To compare the properties of these two domains, we generated two proteins that contained the two LQ sites (Figure 1B), and we studied their interaction with calmodulin. The protein CNGB1-N comprised the N-terminal sequence A<sup>162</sup> to D<sup>264</sup> of rat CNGB1b (MW = 11 640 g/mol). The protein CNGA4-C represented the “C-linker” region of CNGA4 (N<sup>273</sup> to N<sup>351</sup>; MW = 10 150 g/mol), a section of the C-terminus that connects the sixth transmembrane segment to the cAMP-binding site. All proteins contained an N-terminal His-tag that was used for purification purposes. In CNGB1-N, the LQ site resides within a predicted  $\alpha$ -helical region (Figure 1B, asterisks). For CNGA4-C, we obtained no robust prediction for helix formation. As interaction partners, we used wild-type calmodulin as well as the calmodulin mutants  $\text{CaM}^{12}$ ,  $\text{CaM}^{34}$ , and  $\text{CaM}^{1234}$  which lacked functional  $\text{Ca}^{2+}$  binding sites.<sup>26,27,33</sup> The homogeneity of each protein preparation was examined by SDS-PAGE (Figure 2A) and was further supported by far-UV CD spectroscopy (Figure 2B).



Far-UV CD spectra provide information on the relative content of  $\alpha$ -helices,  $\beta$ -sheets, and random-coil structures in a protein. The spectra of CNGB1-N indicate high random-coil content and  $\sim 30\%$   $\alpha$ -helical structure. The CD spectra of CNGA4-C display only little ellipticity, indicating that unordered regions dominate the protein structure. In contrast, all calmodulin spectra displayed a characteristic W-shaped curve, indicating a high content ( $\sim 60\%$ ) of  $\alpha$ -helical structure. The CD spectrum of wild-type CaM revealed the same shape but a lower absolute intensity than the spectra obtained from the CaM mutants. Notwithstanding this discrepancy, the three calmodulin mutants used in this study (CaM<sup>12</sup>, CaM<sup>34</sup>, CaM<sup>1234</sup>) clearly showed W-shaped CD spectra and similar fractions of  $\alpha$ -helical structure. In these mutants, the Ca<sup>2+</sup>-binding sites were disabled by D-to-A mutations in either the N-terminal lobe (CaM<sup>12</sup>), the C-terminal lobe (CaM<sup>34</sup>), or in both lobes (CaM<sup>1234</sup>).

**Binding of Calmodulin to CNGB1-N and CNGA4-C.** To characterize the binding of calmodulin to CNGB1-N and CNGA4-C, we monitored changes in secondary structure using CD spectroscopy. We recorded far-UV spectra for each protein without and with calmodulin. To detect interactions between proteins, we compared spectra recorded from the protein mixtures to hypothetical spectra that were calculated for the case that the proteins did not interact. In the absence of binding, the spectrum obtained from a mixture of channel protein plus calmodulin would correspond to the weighted average spectrum calculated from the experimental spectra of the two individual proteins. In contrast, any difference between the experimental CD spectrum obtained from the protein mixture and the hypothetical spectrum is indicative of protein–protein interactions that are accompanied by changes in the secondary structure.

A Ca<sup>2+</sup>-free solution with equimolar concentrations (20  $\mu$ M) of CNGB1-N and calmodulin yielded a spectrum that did not deviate from the calculated average spectrum of the two components (Figure 3A). However, a clear difference between the two spectra was observed with 30  $\mu$ M Ca<sup>2+</sup> (Figure 3B). Thus, calmodulin binds to CNGB1-N in a Ca<sup>2+</sup>-dependent manner. In olfactory cilia, the Ca<sup>2+</sup> concentration fluctuates between  $\leq 0.1$   $\mu$ M at rest and  $> 1$   $\mu$ M during odor stimulation. Within this Ca<sup>2+</sup> range, calmodulin may be Ca<sup>2+</sup>-free, partially liganded, or fully liganded. To explore the ability of CNGB1-N to bind calmodulin in these three states, we used three different calmodulin mutants in the CD experiments: The mutant CaM<sup>1234</sup> had no intact Ca<sup>2+</sup>-binding site, while the mutants CaM<sup>12</sup> and CaM<sup>34</sup> could bind Ca<sup>2+</sup> at their remaining intact C-terminal or N-terminal lobes, respectively. Thus, we used CaM<sup>12</sup> and CaM<sup>34</sup> at 30  $\mu$ M Ca<sup>2+</sup> to find out whether the channel proteins would bind to partially liganded calmodulin or whether binding required fully liganded calmodulin. We detected no binding of CNGB1-N to the mutant CaM<sup>1234</sup> at 30  $\mu$ M Ca<sup>2+</sup> (Figure 3E), confirming the Ca<sup>2+</sup> dependence of this process. CD experiments with CaM<sup>12</sup> and CaM<sup>34</sup> mutants revealed that CNGB1-N could interact both with CaM<sup>12</sup> and with CaM<sup>34</sup> (Figure 3C,D). Thus, CNGB1-N binds to partially liganded calmodulin, as it occurs at low Ca<sup>2+</sup> concentrations in the unstimulated cell. Similar to CNGB1b-N, an equimolar mixture of CNGA4-C and calmodulin produced a deviation from the calculated average spectrum at 30  $\mu$ M Ca<sup>2+</sup>, but neither in the absence of Ca<sup>2+</sup> nor with the mutant CaM<sup>1234</sup>, indicating Ca<sup>2+</sup>-dependent interaction also with this protein (Figure 3F,G,I). In contrast to CNGB1-N, CNGA4-C interacted neither with CaM<sup>12</sup> nor with CaM<sup>34</sup> (Figure 3H,I). These results suggest that CNGB1-N can permanently interact with calmodulin at low Ca<sup>2+</sup> concentrations in the unstimulated cell, while

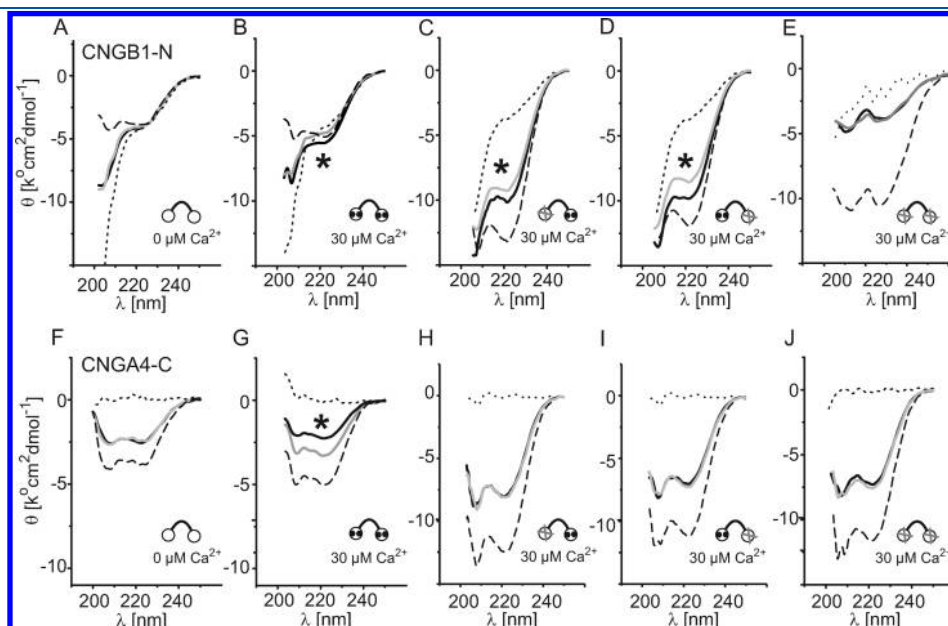


**Figure 3.** Ca<sup>2+</sup> dependency of the CaM interaction with the IQ-type calmodulin binding domains of CNGB1 and CNGA4. Averaged CD spectra ( $n = 3$ ) are shown for 20  $\mu$ M CaM alone (broken line), for the respective test protein at 20  $\mu$ M (dotted line), the weighted average of these spectra (gray line), and for a mixture of 20  $\mu$ M CaM and 20  $\mu$ M test protein (black line). Cherry symbols stand for CaM with black dots indicating bound Ca<sup>2+</sup> ions. Crosses in N- or C-lobes of CaM represent disabled Ca<sup>2+</sup>-binding sites. The asterisk indicates a significant deviation of the calculated spectrum from the measured spectrum of the mixture which is indicative of an interaction between the test protein and calmodulin. (A, F) CD spectra show no interaction of CaM with CNGB1b-N or CNGA4-C in the absence of Ca<sup>2+</sup>, but significant binding in the presence of 30  $\mu$ M Ca<sup>2+</sup> (B, G). Interaction with partially liganded mutants CaM<sup>12</sup> (C, H) and CaM<sup>34</sup> (D, I) was seen only with CNGB1b-N. Neither protein bound to the mutant CaM<sup>1234</sup> (E, J).

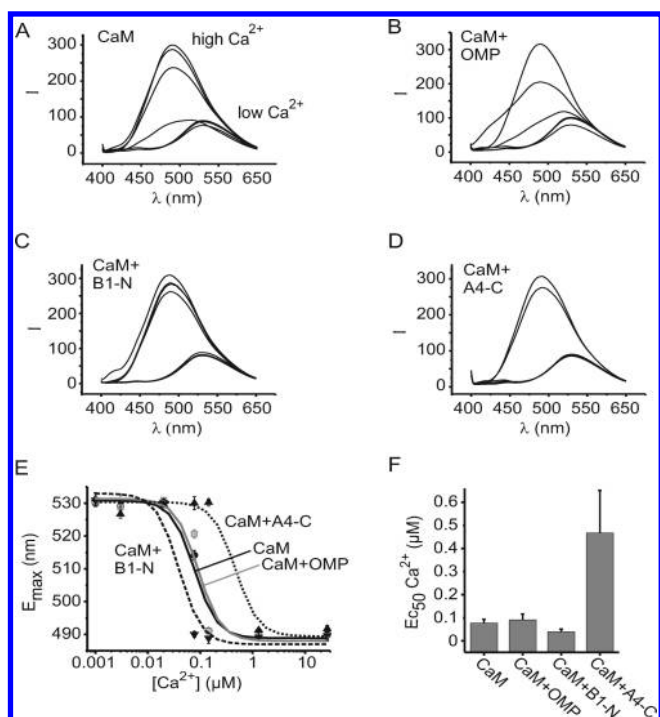


**Figure 4.** Differential effects of CNGB1-N and CNGA4-C on the  $\text{Ca}^{2+}$  sensitivity of calmodulin. Averaged fluorescence emission spectra ( $n = 3-6$ ) at increasing  $\text{Ca}^{2+}$  concentrations (0, 2.9 nM, 19 nM, 77 nM, 140 nM, 1.3  $\mu\text{M}$ , 26.5  $\mu\text{M}$ ).  $I$  = fluorescence intensity. (A) CaM<sup>Badan</sup>, (B) CaM<sup>Badan</sup> + OMP (olfactory marker protein, as control), (C) CaM<sup>Badan</sup> + CNGB1-N, and (D) CaM<sup>Badan</sup> + CNGA4-C. (E) Dose response relationship of the  $\text{Ca}^{2+}$ -dependent blue shift of the emission maximum at increasing  $\text{Ca}^{2+}$  concentrations.  $E_{\text{max}}$  = emission maximum (F).  $\text{EC}_{50}$  values of the  $\text{Ca}^{2+}$ -dependent blue shift (means of 3–6 measurements): CaM<sup>Badan</sup>  $75 \pm 15$  nM, CaM<sup>Badan</sup> + OMP  $88 \pm 26$  nM, CaM<sup>Badan</sup> + CNGB1-N  $39 \pm 12$  nM, CaM<sup>Badan</sup> + CNGA4-C  $467 \pm 18$  nM.

CNGA4-N binds calmodulin only at elevated intracellular  $\text{Ca}^{2+}$  concentrations when calmodulin is fully liganded.

**$\text{Ca}^{2+}$  Sensitivity of Calmodulin.** The  $\text{Ca}^{2+}$  sensitivity of calmodulin often changes when  $\text{Ca}^{2+}$ -calmodulin binds to a target protein. To determine the  $\text{Ca}^{2+}$  sensitivity of calmodulin with and without the test proteins, we tagged calmodulin with the conformation-sensitive fluorescent dye Badan (“CaM<sup>Badan</sup>”).<sup>34</sup> This dye reports conformational changes of the calmodulin molecule that are induced by  $\text{Ca}^{2+}$  binding. We coupled Badan covalently to the cysteine residue of CaM<sup>T33C</sup> and monitored the  $\text{Ca}^{2+}$ -dependent conformational change of CaM<sup>Badan</sup> through a blue shift of the fluorescence maximum (Figure 4A). The  $\text{Ca}^{2+}$  dependence of this blue shift was little affected by a small control protein (OMP) which binds neither  $\text{Ca}^{2+}$  nor calmodulin (Figure 4B). In contrast, both CNGB1-N (Figure 4C) and CNGA4-C (Figure 4D) changed the  $\text{Ca}^{2+}$  dependence of the CaM<sup>Badan</sup> fluorescence. Quantitative evaluation of the data yielded an  $\text{EC}_{50}$  for  $\text{Ca}^{2+}$  binding to CaM<sup>Badan</sup> of 77 nM  $\text{Ca}^{2+}$  without proteins and 90 nM  $\text{Ca}^{2+}$  for the control protein OMP. CNGB1-N reduced the  $\text{EC}_{50}$  to 39 nM  $\text{Ca}^{2+}$ , and CNGA4-C increased  $\text{EC}_{50}$  to 429 nM  $\text{Ca}^{2+}$  (Figure 4E,F). All test proteins were added to CaM<sup>Badan</sup> at a molar ratio of 2:1. These results demonstrate that binding of CNGB1-N is favored at low  $\text{Ca}^{2+}$  concentrations while the association of CNGA4-C with calmodulin requires elevated  $\text{Ca}^{2+}$  levels.

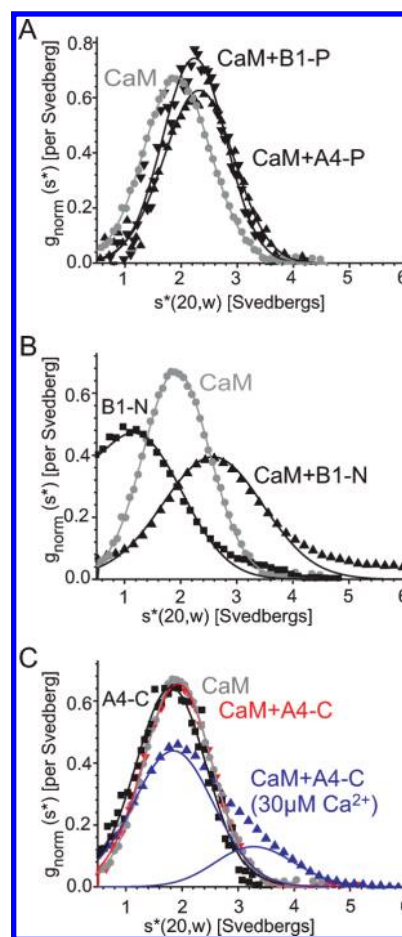


**Figure 5.** Sedimentation velocity analysis by analytical ultracentrifugation at saturating  $\text{Ca}^{2+}$  concentrations. (A) Sedimentation velocity analysis of CaM and of 2:1 molar mixtures of the peptides CNGB1-P and CNGA4-P with CaM. The maxima of the curves correspond to the best-fit  $s$  values [S], with 1.95 S for CaM, 2.25 S for CaM + CNGB1-P, and 2.24 S for CaM + CNGA4-P. All curves represent ideal normal distributions, indicating the formation of a ternary complex consisting of two peptides plus one calmodulin molecule. (B) Sedimentation velocity analysis of CNGB1-N and of a 2:1 molar mixture with CaM. Best-fit  $s$  values [S] are 1.95 S for CaM (ideal normal distribution), 1.35 S for CNGB1-N (80%) beside some oligomers, and 2.66 S for the CaM–CNGB1-N complex (80%). No evidence was found for complex formation with two calmodulin molecules at an expected sedimentation velocity of  $>4.5$  S. (C) Sedimentation velocity analysis of CNGA4-C and 2:1 molar mixtures with CaM. Best-fit  $s$  values [S] are 1.95 S for CaM and 1.88 S for CNGA4-C (both ideal normal distributions); 1.93 S for 2:1 mixtures; 1.95 S (80%) and 3.38 S (20%) for 2:1 mixtures in 30  $\mu\text{M}$   $\text{Ca}^{2+}$ . No evidence was detected for complex formation with two calmodulin molecules ( $>4$  S).

**Formation of the Regulatory Complex.** To find out whether the protein complexes between calmodulin and our binding-site proteins contained one or two calmodulin molecules, we performed sedimentation velocity experiments in an analytical ultracentrifuge. We determined the sedimentation coefficients of the test proteins alone as well as those of complexes in protein mixtures at a saturating  $\text{Ca}^{2+}$  concentration (1 mM). The distribution of sedimentation coefficients reflects size and shape distributions of proteins, thus allowing indirect determination of the stoichiometry of homo- and hetero-oligomers. A previous NMR study has demonstrated that a 26-residue peptide

containing the LQ site of CNGB1 binds calmodulin at a ratio of 2:1.<sup>35</sup> We started by examining this finding using analytical ultracentrifugation with each peptide, CNGB1-P and CNGA4-P (Figure 1B), and calmodulin at 2:1 molar ratios. Sedimentation velocity analysis showed that all curves could be fitted with single ideal sedimenting species with peak *s* values of 1.95 S for calmodulin, 2.25 S for calmodulin + CNGB1b-P, and 2.24 S for calmodulin + CNGA4-P (Figure 5A). The peak shifts in the mixtures could be explained with the formation of a ternary complex consisting of two peptides plus one calmodulin molecule. Thus, our data are consistent with the NMR results and confirm that each calmodulin molecule binds two binding-site peptides.

However, binding of calmodulin to a peptide can differ dramatically from binding of the same peptide sequence embedded in a larger protein environment. To test this, we examined the sedimentation velocities of the protein CNGB1-N without and with calmodulin at a 2:1 molar ratio (18  $\mu$ M CNGB1-N + 9  $\mu$ M calmodulin) (Figure 5B). The calmodulin curve represents an ideal normal distribution with a peak *s* value of 1.95 S, indicating a highly homogeneous protein species. For CNGB1b-N, the fit indicated that about 80% sedimented at a monomeric state at 1.35 S. The sedimentation coefficient for the 2:1 mix was 2.66 S for the complex, giving a fraction of bound calmodulin of 80%. There was no evidence for complex formation with two calmodulin molecules at an expected sedimentation velocity of >4.5 S.

The analysis of the CNGA4-C protein yielded an ideal normal distribution, indicating a highly homogeneous protein species with a peak *s* value of 1.88 S (Figure 5C). The observation that the *s* value of CNGA4-C was somewhat higher than that of CNGB1b-N may indicate that CNGA4-C exists in a largely unfolded conformation as suggested by CD spectroscopy. Calmodulin was again fitted with a peak *s* value of 1.95 S. In 2:1 mixtures (18  $\mu$ M CNGA4-C + 9  $\mu$ M calmodulin) the curve could be fitted with a single peak *s* value of 1.93 S, indicating that both proteins do not form a complex under these conditions. Interestingly, decreasing the  $\text{Ca}^{2+}$  concentration to 30  $\mu$ M yielded a curve with a maximum at 2.20 S, which could be fitted with two distinct peak *s* values at 1.95 S (80%) and at 3.38 S (20%) (blue lines). Thus, about 20% of calmodulin in this mix was bound to CNGA4-C. No evidence was detected for complex formation with two calmodulin molecules (>4 S).

This sedimentation study revealed two important points: (1) The CNGB1-N/calmodulin complex contains only a single calmodulin molecule; (2) at saturating  $\text{Ca}^{2+}$  levels, CNGB1-N binds to calmodulin much more efficiently than CNGA4-C.

## DISCUSSION

**Comparison of the LQ-Type Calmodulin Binding Sites in CNGA4 and CNGB1.** The present analysis of calmodulin binding was conducted to complement a series of patch-clamp studies on the feedback inhibition of the olfactory cAMP-gated channel. The electrophysiological data indicated that the heteromeric channel (2 CNGA2 + 1 CNGA4 + 1 CNGB1b) responds to  $\text{Ca}^{2+}$ -calmodulin with a rapid right shift of its dose–response relation for cAMP. This desensitization was observed both in membrane patches excised from olfactory receptor neurons<sup>18,21,23,36</sup> and in heteromeric recombinant channels coassembled from the three different subunits.<sup>21,22,37</sup> The functional studies also revealed that calmodulin is constitutively associated with the olfactory channel,<sup>21</sup> serving as a built-in  $\text{Ca}^{2+}$  sensor for the feedback-control

mechanism that limits the activation time of this channel.<sup>11,12,38</sup> However, the channel electrophysiology also produced conflicting evidence about the calmodulin-binding sites involved in feedback control. The N-terminal calmodulin-binding site of CNGA2 can be removed from the channel without compromising feedback inhibition.<sup>21</sup> In contrast, the N-terminal LQ site of CNGB1b is necessary for this process, as deletion of this site, or the introduction of an L-to-E exchange, completely eliminates feedback inhibition of the channel in membrane patches excised from transfected HEK 293 cells<sup>21</sup> or from olfactory receptor neurons of genetically altered CNGB1b<sup>−/−</sup>-mice.<sup>23</sup> Results on the role of CNGA4 are less conclusive. They indicate that this subunit is not involved in inhibition when channels are allowed to retain cytosolic material at their intracellular side.<sup>25</sup> If, however, this material is washed off for 10 min in  $\text{Ca}^{2+}$ -free solution, the channels become sensitive to an L-to-E mutation in the LQ site of CNGA4.

The binding studies reported here confirm the characteristic features of calmodulin binding to CNGB1b that were first observed in the functional studies. The C-terminal LQ site of this subunit binds to calmodulin at  $\text{Ca}^{2+}$  concentrations below 0.1  $\mu$ M, but not at in the absence of  $\text{Ca}^{2+}$ . This is consistent with results from patch-clamp experiments where calmodulin was stably associated with the channel at 0.1  $\mu$ M  $\text{Ca}^{2+}$  but was washed off in  $\text{Ca}^{2+}$ -free solution.<sup>21,36</sup> The CNGB1b LQ site binds even if only one lobe of calmodulin is able to bind  $\text{Ca}^{2+}$ . This leaves the other lobe free for a second type of interaction, possibly the binding to a target site that desensitizes the channel. The agreement between the functional results on the permanently attached calmodulin and the CNGB1b-N binding studies presented here strongly suggests that the CNGB1b LQ site is the anchoring point that keeps calmodulin tethered to the channel. The regulatory target site still needs to be identified.

The LQ site contained in CNGA4-C seems not able to perform two distinct functions. It requires much higher  $\text{Ca}^{2+}$  concentrations for binding, too high for constitutive association. Moreover, since both lobes of calmodulin must be  $\text{Ca}^{2+}$ -loaded for binding to CNGA4-C, there can be no dual effect on two spatially separated sites on this subunit. Finally, in the analytical ultracentrifuge, a weak interaction with calmodulin could be observed only in 30  $\mu$ M  $\text{Ca}^{2+}$ , indicating the limited propensity of this protein for complex formation with calmodulin. Taken together, our binding data demonstrate that the C-linker of CNGA4 has much less favorable properties for interaction with calmodulin than the N-terminus of CNGB1b. Our data obtained with protein fragments containing the CaM-binding domains are in accordance with the finding that full-length CNGA4 does not contribute to feedback inhibition of the olfactory channel.<sup>25</sup> Thus, CNGB1b appears to be the only calmodulin-responsive subunit in the olfactory channel. For a direct evaluation of the binding process in the native channel, other methods are required.

**Implications for the Concept of CNG Channel Regulation by  $\text{Ca}^{2+}$ -Calmodulin.** Currently available data indicate that it is always a B-subunit that confers  $\text{Ca}^{2+}$ -calmodulin sensitivity to the various CNG channels. Although all subunits possess calmodulin-binding site motifs, and despite the occurrence of  $\text{Ca}^{2+}$ -calmodulin effects on homomeric CNGA2 channels, the native, heteromeric channels respond to  $\text{Ca}^{2+}$  signals through their B subunits. The N-terminal LQ site of the two CNGB1 splice variants—CNGB1a in rod photoreceptors and CNGB1b in olfactory receptor neurons—appears to provide the structural basis for feedback inhibition. A mechanistic concept for this



process was first developed for the rod photoreceptor channel that contains a single CNGB1a subunit. The N-terminus of CNGB1a binds to the C-terminus of CNGA1,<sup>39</sup> and this interaction is considered necessary to maintain a high ligand sensitivity of these channels. Calmodulin disrupts this interdomain interaction and desensitizes the channel by binding to the LQ-type site. This notion is supported by time-resolved FRET measurements which revealed that channel inhibition and interdomain separation proceed simultaneously.<sup>40</sup> The same concept was transferred to olfactory channels. Indeed, the cAMP sensitivity of homomeric CNGA2 channels seems to be regulated in a similar way: Calmodulin binds to the N-terminal 1–5–8–14-type binding site and separates interactions between the N- and C-termini of the CNGA2 homomer.<sup>39</sup> However, calmodulin can bind to CNGA2 homomers only when the channels are closed, while the binding to heteromeric olfactory channels is not state-dependent.<sup>22</sup> It is, therefore, unlikely that the same principle of channel inhibition operates in homomers and heteromers. Earlier studies of a mouse model where CNGA4 was genetically ablated suggested an involvement of this subunit in calmodulin-mediated channel desensitization.<sup>41,42</sup> This was supported by kinetic measurements of recombinant olfactory channels, which indicated that CNGA4 was necessary for a rapid and state-independent response to Ca<sup>2+</sup>-calmodulin.<sup>22</sup> More recent work has shown that both approaches are problematic. First, CNGA4 is needed for targeting the other two subunits to the sensory cilia. Immunohistochemistry of the olfactory epithelium from CNGA4<sup>−/−</sup> mouse detected no expression of CNGA2 and CNGB1b in the cilia.<sup>43</sup> The data from the CNGA4<sup>−/−</sup> mouse are, therefore, difficult to interpret. They may originate in part from residual CNGA2 homomers with their different calmodulin response. Second, recombinant olfactory CNG channels in the *in vitro* situation of an inside-out patch without cytosolic material behave differently from channels in contact with the cell.<sup>25</sup> Results from such experiments have to be treated with caution as channels *in vitro* may respond to calmodulin in a way different from native channels. Thus, our binding data support the concept that a single lobe of calmodulin is permanently associated with the LQ site located in the N-terminus of the CNGB1b subunit. The second lobe is poised to bind to an as yet unidentified regulatory site at elevated Ca<sup>2+</sup> concentrations. In contrast, the LQ site of CNGA4 is not able to attach calmodulin permanently to the channel, binds calmodulin with low efficiency, and is probably not involved in channel regulation by Ca<sup>2+</sup>-calmodulin.

In conclusion, among nine different calmodulin-binding motifs in the CNG-channel family (Figure 1A), the LQ site of CNGB1 subunits is the only domain for which a consistent set of binding data and physiological data support a role in channel regulation.

## AUTHOR INFORMATION

### Corresponding Author

\*Phone: +49 6221 545887. Fax: +49 6221 545627. E-mail: moehrlen@uni-hd.de.

### Funding Sources

This work was supported by the Deutsche Forschungsgemeinschaft, Germany (MO 1384/1 to F.M. and S.F.).

## ABBREVIATIONS

BADAN, 6-bromoacetyl-2-dimethylaminonaphthalene; CaM, calmodulin; cAMP, cyclic adenosine monophosphate; CD,

circular dichroism; cGMP, cyclic guanosine monophosphate; CNG, cyclic nucleotide-gated; OMP, olfactory marker protein.

## REFERENCES

- (1) Kaupp, U. B., and Seifert, R. (2002) Cyclic nucleotide-gated ion channels. *Physiol. Rev.* 82, 769–824.
- (2) Matulef, K., and Zagotta, W. N. (2003) Cyclic nucleotide-gated ion channels. *Annu. Rev. Cell Dev. Biol.* 19, 23–44.
- (3) Pifferi, S., Boccaccio, A., and Menini, A. (2006) Cyclic nucleotide-gated ion channels in sensory transduction. *FEBS Lett.* 580, 2853–2859.
- (4) Biel, M., and Michalakakis, S. (2007) Function and dysfunction of CNG channels: insights from channelopathies and mouse models. *Mol. Neurobiol.* 35, 266–277.
- (5) Biel, M., and Michalakakis, S. (2009) Cyclic nucleotide-gated channels. *Handb. Exp. Pharmacol.* 111–136.
- (6) Zheng, J., Trudeau, M. C., and Zagotta, W. N. (2002) Rod cyclic nucleotide-gated channels have a stoichiometry of three CNGA1 subunits and one CNGB1 subunit. *Neuron* 36, 891–896.
- (7) Zhong, H., Molday, L. L., Molday, R. S., and Yau, K. W. (2002) The heteromeric cyclic nucleotide-gated channel adopts a 3A:1B stoichiometry. *Nature* 420, 193–198.
- (8) Peng, C., Rich, E. D., and Varnum, M. D. (2004) Subunit configuration of heteromeric cone cyclic nucleotide-gated channels. *Neuron* 42, 401–410.
- (9) Zheng, J., and Zagotta, W. N. (2004) Stoichiometry and assembly of olfactory cyclic nucleotide-gated channels. *Neuron* 42, 411–421.
- (10) Fain, G. L., Matthews, H. R., Cornwall, M. C., and Koutalos, Y. (2001) Adaptation in vertebrate photoreceptors. *Physiol. Rev.* 81, 117–151.
- (11) Matthews, H. R., and Reiser, J. (2003) Calcium, the two-faced messenger of olfactory transduction and adaptation. *Curr. Opin. Neurobiol.* 13, 469–475.
- (12) Menini, A. (1999) Calcium signalling and regulation in olfactory neurons. *Curr. Opin. Neurobiol.* 9, 419–426.
- (13) Dzeja, C., Hagen, V., Kaupp, U. B., and Frings, S. (1999) Ca<sup>2+</sup> permeation in cyclic nucleotide-gated channels. *EMBO J.* 18, 131–144.
- (14) Seifert, R., Eismann, E., Ludwig, J., Baumann, A., and Kaupp, U. B. (1999) Molecular determinants of a Ca<sup>2+</sup>-binding site in the pore of cyclic nucleotide-gated channels: S5/S6 segments control affinity of intrapore glutamates. *EMBO J.* 18, 119–130.
- (15) Zheng, J., Varnum, M. D., and Zagotta, W. N. (2003) Disruption of an intersubunit interaction underlies Ca<sup>2+</sup>-calmodulin modulation of cyclic nucleotide-gated channels. *J. Neurosci.* 23, 8167–8175.
- (16) Trudeau, M. C., and Zagotta, W. N. (2003) Calcium/calmodulin modulation of olfactory and rod cyclic nucleotide-gated ion channels. *J. Biol. Chem.* 278, 18705–18708.
- (17) Trudeau, M. C., and Zagotta, W. L. N. (2004) Dynamics of Ca<sup>2+</sup>-calmodulin-dependent inhibition of rod cyclic nucleotide-gated channels measured by patch-clamp fluorometry. *J. Gen. Physiol.* 124, 211–223.
- (18) Chen, T. Y., and Yau, K. W. (1994) Direct modulation by Ca(2+)-calmodulin of cyclic nucleotide-activated channel of rat olfactory receptor neurons. *Nature* 368, 545–548.
- (19) Liu, M. Y., Chen, T. Y., Ahamed, B., Li, J., and Yau, K. W. (1994) Calcium-Calmodulin Modulation of the Olfactory Cyclic Nucleotide-Gated Cation Channel. *Science* 266, 1348–1354.
- (20) Kramer, R. H., and Siegelbaum, S. A. (1992) Intracellular Ca<sup>2+</sup> regulates the sensitivity of cyclic nucleotide-gated channels in olfactory receptor neurons. *Neuron* 9, 897–906.
- (21) Bradley, J., Bönigk, W., Yau, K. W., and Frings, S. (2004) Calmodulin permanently associates with rat olfactory CNG channels under native conditions. *Nature Neurosci.* 7, 705–710.
- (22) Bradley, J., Reuter, D., and Frings, S. (2001) Facilitation of calmodulin-mediated odor adaptation by cAMP-gated channel subunits. *Science* 294, 2176–2178.



- (23) Song, Y., Cygnar, K. D., Sagdullaev, B., Valley, M., Hirsh, S., Stephan, A., Reisert, J., and Zhao, H. (2008) Olfactory CNG channel desensitization by  $\text{Ca}^{2+}$ /CaM via the B1b subunit affects response termination but not sensitivity to recurring stimulation. *Neuron* 58, 374–386.
- (24) Cheney, R. E., and Mooseker, M. S. (1992) Unconventional myosins. *Curr. Opin. Cell Biol.* 4, 27–35.
- (25) Waldeck, C., Vocke, K., Ungerer, N., Frings, S., and Möhrle, F. (2009) Activation and desensitization of the olfactory cAMP-gated transduction channel: identification of functional modules. *J. Gen. Physiol.* 134, 397–408.
- (26) Erickson, M. G., Alseikhan, B. A., Peterson, B. Z., and Yue, D. T. (2001) Preassociation of calmodulin with voltage-gated  $\text{Ca}^{2+}$  channels revealed by FRET in single living cells. *Neuron* 31, 973–985.
- (27) Keen, J. E., Khawaled, R., Farrens, D. L., Neelands, T., Rivard, A., Bond, C. T., Janowsky, A., Fakler, B., Adelman, J. P., and Maylie, J. (1999) Domains responsible for constitutive and  $\text{Ca}^{2+}$ -dependent interactions between calmodulin and small conductance  $\text{Ca}^{2+}$ -activated potassium channels. *J. Neurosci.* 19, 8830–8838.
- (28) Owenius, R., Osterlund, M., Lindgren, M., Svensson, M., Olsen, O. H., Persson, E., Freskgård, P. O., and Carlsson, U. (1999) Properties of spin and fluorescent labels at a receptor-ligand interface. *Biophys. J.* 77, 2237–2250.
- (29) Williams, D. A., and Fay, F. S. (1990) Intracellular calibration of the fluorescent calcium indicator Fura-2. *Cell Calcium* 11, 75–83.
- (30) Brahms, S., and Brahms, J. (1980) Determination of protein secondary structure in solution by vacuum ultraviolet circular dichroism. *J. Mol. Biol.* 138, 149–178.
- (31) Weitz, D., Zoche, M., Müller, F., Beyermann, M., Korschen, H. G., Kaupp, U. B., and Koch, K. W. (1998) Calmodulin controls the rod photoreceptor CNG channel through an unconventional binding site in the N-terminus of the beta-subunit. *EMBO J.* 17, 2273–2284.
- (32) Peng, C., Rich, E. D., Thor, C. A., and Varnum, M. D. (2003) Functionally important calmodulin-binding sites in both NH<sub>2</sub>- and COOH-terminal regions of the cone photoreceptor cyclic nucleotide-gated channel CNGB3 subunit. *J. Biol. Chem.* 278, 24617–24623.
- (33) Kaneko, H., Möhrle, F., and Frings, S. (2006) Calmodulin contributes to gating control in olfactory calcium-activated chloride channels. *J. Gen. Physiol.* 127, 737–748.
- (34) Gangopadhyay, J. P., Grabarek, Z., and Ikemoto, N. (2004) Fluorescence probe study of  $\text{Ca}^{2+}$ -dependent interactions of calmodulin with calmodulin-binding peptides of the ryanodine receptor. *Biochem. Biophys. Res. Commun.* 323, 760–768.
- (35) Orsale, M., Melino, S., Contessa, G. M., Torre, V., Andreotti, G., Motta, A., Paci, M., Desideri, A., and Cicero, D. O. (2003) Two distinct calcium-calmodulin interactions with N-terminal regions of the olfactory and rod cyclic nucleotide-gated channels characterized by NMR spectroscopy. *FEBS Lett.* 548, 11–16.
- (36) Balasubramanian, S., Lynch, J. W., and Barry, P. H. (1996) Calcium-dependent modulation of the agonist affinity of the mammalian olfactory cyclic nucleotide-gated channel by calmodulin and a novel endogenous factor. *J. Membr. Biol.* 152, 13–23.
- (37) Brady, J. D., Rich, E. D., Martens, J. R., Karpen, J. W., Varnum, M. D., and Brown, R. L. (2006) Interplay between PIP<sub>3</sub> and calmodulin regulation of olfactory cyclic nucleotide-gated channels. *Proc. Natl. Acad. Sci. U.S.A.* 103, 15635–15640.
- (38) Bradley, J., Reisert, J., and Frings, S. (2005) Regulation of cyclic nucleotide-gated channels. *Curr. Opin. Neurobiol.* 15, 343–349.
- (39) Varnum, M. D., and Zagotta, W. N. (1997) Interdomain interactions underlying activation of cyclic nucleotide-gated channels. *Science* 278, 110–113.
- (40) Trudeau, M. C., and Zagotta, W. N. (2004) Dynamics of  $\text{Ca}^{2+}$ -calmodulin-dependent inhibition of rod cyclic nucleotide-gated channels measured by patch-clamp fluorometry. *J. Gen. Physiol.* 124, 211–223.
- (41) Munger, S. D., Lane, A. P., Zhong, H., Leinders-Zufall, T., Yau, K. W., Zufall, F., and Reed, R. R. (2001) Central role of the CNGA4 channel subunit in  $\text{Ca}^{2+}$ -calmodulin-dependent odor adaptation. *Science* 294, 2172–2175.
- (42) Kelliher, K. R., Ziesmann, J., Munger, S. D., Reed, R. R., and Zufall, F. (2003) Importance of the CNGA4 channel gene for odor discrimination and adaptation in behaving mice. *Proc. Natl. Acad. Sci. U.S.A.* 100, 4299–4304.
- (43) Michalak, S., Reisert, J., Geiger, H., Wetzel, C., Zong, X., Bradley, J., Spehr, M., Hüttel, S., Gerstner, A., Pfeifer, A., Hatt, H., Yau, K. W., and Biel, M. (2006) Loss of CNGB1 protein leads to olfactory dysfunction and subunitary cyclic nucleotide-gated channel trapping. *J. Biol. Chem.* 281, 35156–35166.
- (44) Combet, C., Blanchet, C., Geourjon, C., and Deleage, G. (2000) NPS@: network protein sequence analysis. *Trends Biochem. Sci.* 25, 147–150.